Physica B 149 (1988) 293-305
North-Holland, Amsterdam

MAGNETISM AND SPIN FLUCTUATIONS OF LAVES PHASE MANGANESE COMPOUNDS

M. SHIGA
Department of Metal Science and Technology, Kyoto University, Sakyo-ku, Kyoto 606, Japan

The magnetism of Laves phase compounds RMn_2 is reviewed. The conditions for the onset of Mn moments and the type of spin fluctuations of the Mn sublattice are discussed. It is shown that the Mn moments, if they exist, are unstable and easily collapse on raising the temperature or on substituting R or Mn by a third element with a smaller atomic volume. By analyzing the thermal expansion curves, the amplitudes of spin fluctuations in YMn_2 and related compounds are estimated.

1. Introduction

Laves phase intermetallic compound AB_2 is one of the most popular intermetallic compounds containing transition metals. There are two types of crystal structures of C15 (cubic Laves) and C14 (hexagonal Laves) as shown in fig. 1. The interrelation between these two structures is similar to that between fcc and hcp, i.e., a different order of packings of atomic layers. Therefore, the coordination number is the same for both structures. Numerous compounds exist depending upon the combinations of A and B elements. Among them, the compounds AT_2, where T stands for a 3*d* transition metal, are interesting in respect of magnetism. One of the characteristics of this structure is that the nearest neighbor of a B atom is also a B atom and the atomic distance between the transition metals in AT_2 and hence the width of 3*d* band are nearly the same as that of pure 3*d* metals.

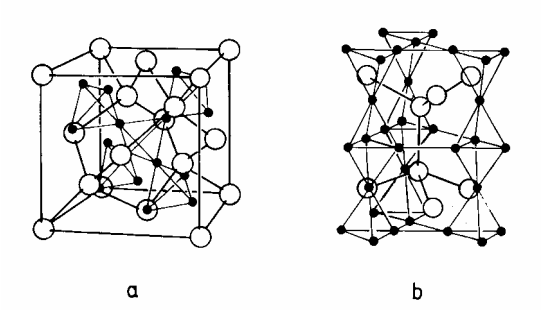

Fig. 1. Crystal structures of Laves phase compounds, AB_2. a) C15 (cubic). b) C14 (hexagonal). Open circles stand for A atoms and closed circles for B atoms.

Therefore, it is possible to control the band width or the Fermi level by choosing an appropriate A element, finding many types of magnetism. Furthermore, making a pseudo-binary compound like $(A_{1-x}A'_x)T_2$, We Can Change conditions for the onset of magnetism without disturbing the band structure so much. So far, extensive studies have been done for Laves phase compounds in many respects, including the band calculations by Prof. Shimizu's school [1-3]. In this review article, we are concerned with RMn_2 compounds in respect of spin fluctuations and magnetovolume effects.

2. Spin fluctuations and magnetovolume effects

Recent developments in the theory of spin fluctuations give us a unified picture of the magnetism of transition metals and alloys ranging from weakly itinerant electron ferro- or antiferromagnetism to local moment systems [4]. One of the most important quantities characterizing the magnetism of a particular metal is the amplitude of local spin fluctuations, S_L^2, and its temperature dependence. Typical features of the spin fluctuations are shown in fig. 2, where the vertical axis represents the square amplitude of local spin fluctuations, that is the magnitude of the local magnetic moment. From a to e, the electron-electron correlation energy increases. The curve a represents a Pauli paramagnet, b an exchange enhanced Pauli paramagnet, c a weakly itinerant electron ferro-(or antiferro-)magnet and e the local moment limit. The curve corresponds to an Invar-type

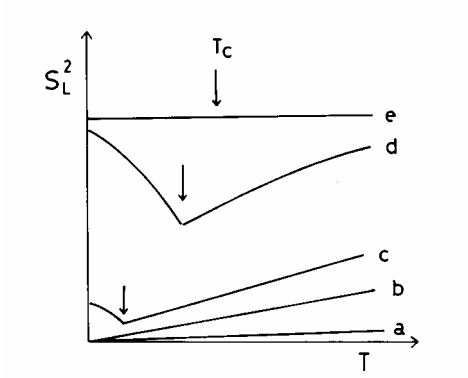

Fig. 2. Temperature. dependence of the amplitude of spin fluctuations. a) Pauli paramagnet. b) Nearly ferro-(or antiferro-)magnetic. c) Weakly ferromagnetic. d) Invar type. e: Local moment limit.

alloy, where S_L^2 changes substantially with temperature. An actual metal locates somewhere in this schematic representation. However, it is not easy to estimate the temperature dependence of S_L^2. Neutron scattering measurements may be the best method to estimate S_L^2. However, scanning of a wide range of the momentum and energy space is necessary for a reliable estimation of S_L^2, which is hardly attained in the present neutron facilities.

We have pointed out through analyses of the lattice parameter of 3*d* metal alloys that the atomic volume of 3d atoms expands when they are magnetized [5, 6]. The magnitude of the expansion is given by $\Delta V/V = \omega_m \sim k m_L^2$. The proportionality constant, k, is roughly 10^{-2} per μ_B^2. When m_L^2, that is $(2\mu_B S_L)^2$, varies with temperature, a thermal expansion anomaly is observed. Therefore, analyzing the thermal expansion curves properly, we can estimate the temperature dependence of S_L^2.

For the cases a - e, shown in fig. 2, the thermal expansion curves of a Pauli paramagnet, a, and the local moment limit, e, show normal behavior due to lattice vibrations. On the other hand, an exchange enhanced Pauli paramagnet, b, and a weakly itinerant ferromagnet above T_c should have an enhanced thermal expansion coefficient(TEC) [7-9]. The negative thermal expansion coefficient observed in weakly itinerant ferromagnets and the large spontaneous volume magnetostriction of Invar-type alloys are explained by a reduction of S_L^2 with increasing temperature up to T_c [10]. We will show in this article that every case is realized in the series of RMn_2 and related compounds.

3. YMn_2: An itinerant electron antiferromagnet

The magnetic susceptibility of YMn_2 increases monotonically with increasing temperature except for a tiny anomaly around 100 K and at low temperatures, indicating Pauli paramagnetism (fig. 3). We found, however, that there is a huge volume change of about 5% around 100 K as shown in fig. 4 [11, 12]. By neutron diffraction and NMR measurements, it has been revealed that this compound is an antiferromagnet with a Mn moment of 2.7 μ_B and $T_N \sim 100$ K [13], of which magnetic structure is shown in fig. 5. The magnetic transition is of the first order with a large thermal hysteresis of about 30 K. Recently, the magnetic structure of YMn_2 has been reexamined by using long-wavelength neutrons and it has been shown that the antiferromagnetic structure is helically modulated with a period of about 400 Å[14]. The zero field NMR spectrum of YMn_2 consists of two peaks with the intensity ratio of 3:1, which is ascribed to anisotropic hyperfine interactions for a spin direction of (111) [13]. Therefore, the modulation of spin directions is not simply helical but something like rectangular waves. So far, the exact spin structure is not yet fixed.

With respect to spin fluctuations, the temperature dependence of susceptibility above T_N indicates itinerant electron magnetism. The large volume shrinkage at T_N may be ascribed to the collapse of Mn moment of $2.7\mu_B$ of the antiferromagnetic phase. Furthermore, one should note that the TEC above T_N is abnormally large, being 50 x 10^{-6}, and shows a trend to decrease at high temperatures. This enhancement of the TEC will be explained as a result of thermal excitations of spin fluctuations in a later section. The temperature dependence of the susceptibility of YMn_2 has been calculated on the basis of band calculations, giving a good agreement with the experiment [1].

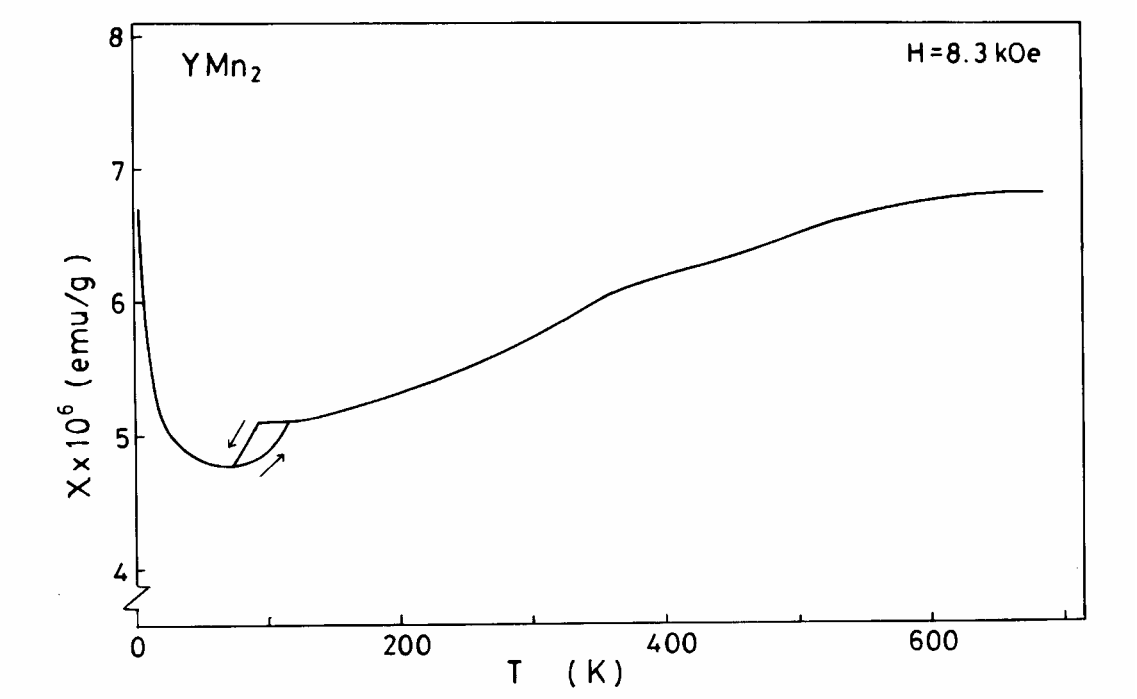

Fig. 3. Temperature dependence of the magnetic susceptibility of YMn_2.

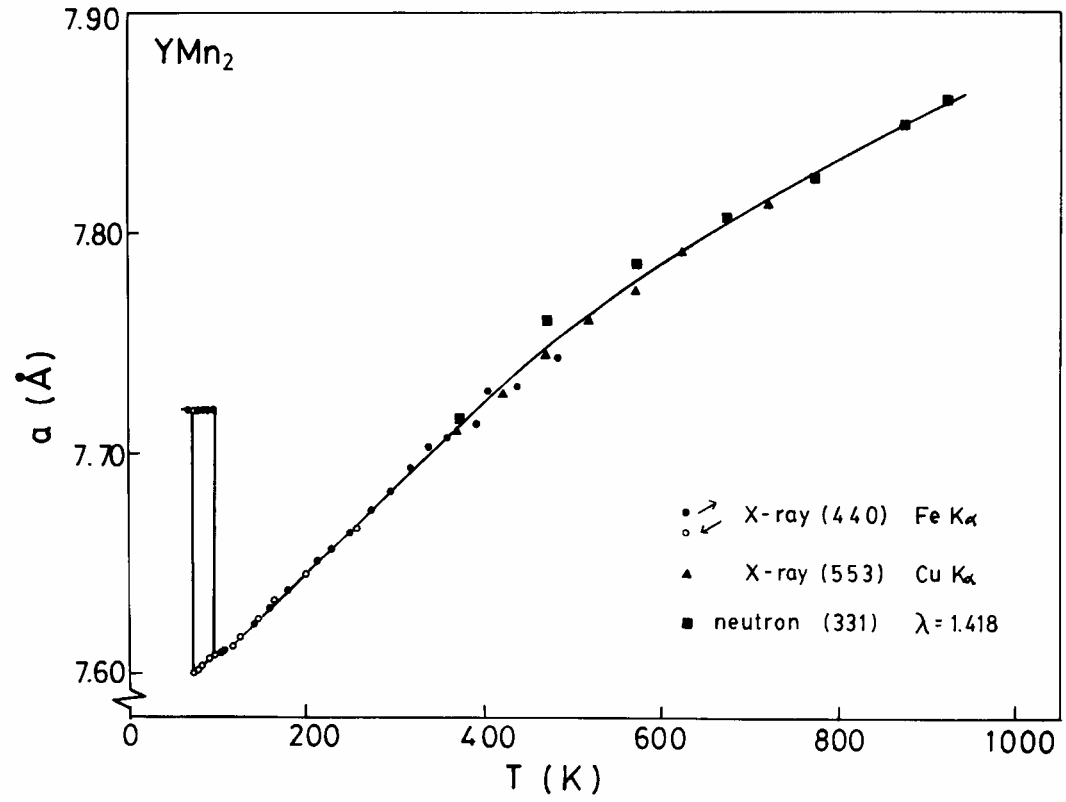

Fig. 4. Temperature dependence of the lattice parameter of YMn_2.

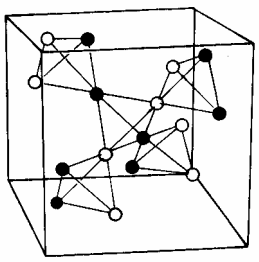

Fig. 5. Spin structure of YMn_2. Only Mn sites are shown. Open and closed circles represent Mn atoms with up and down spins. A recent neutron diffraction study has revealed that this antiferromagnetic spin arrangement is helically modulated with a period of about 400 Å. (see text.)

4. Magnetism of RMn_2

4.1. Mn atomic moment

Magnetism of RMn_2 (R: rare earth) series has not yet been established because of the complexity of magnetic structure. Of course, R atoms have well-defined localized moments but it is not clear whether Mn has a magnetic moment or not. In fig. 6, the thermal expansion curves of RMn_2 are shown. As seen in the figure, except for $HoMn_2$, $ErMn_2$. and $DyMn_2$, they exhibit similar thermal expansion curves characterized by an expansion of the lattice below around 100 K, indicating the onset of Mn moments. On the other hand, the zero-field NMR spectra of ^{55}Mn has shown that the hyperfine fields at ^{55}Mn nuclei in $HoMn_2$ and $ErMn_2$ are exceptionally smaller than those of other RMn_2 compounds [15]. By separating the hyperfine field due to the Mn moment itself and the transferred hyperfine field from R moments, Yoshimura *et al*. have estimated the magnitude of Mn moment [15]. The results are plotted in fig. 7 as a function of the lattice parameter at 4.2 K (for C14, $(\sqrt{3}a^2c)^{1/3}$). From these observations, it can be concluded that the Mn atom has a large (2 - 3μ_B) magnetic moment in the ground state in RMn_2 except in $ErMn_2$, $HoMn_2$ and $DyMn_2$ and that it collapses or is substantially reduced at the magnetic transition temperature (corresponding to the case d of fig. 2).

It is an interesting problem to find the factor

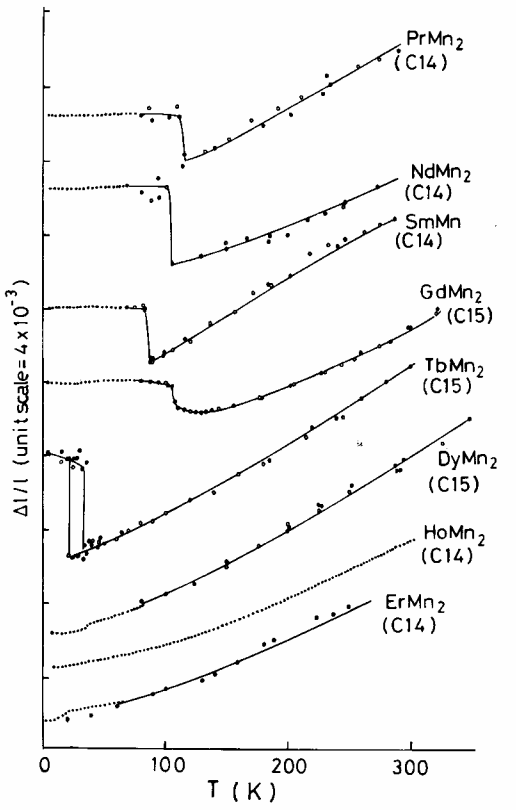

Fig. 6. Thermal expansion curves of RMn_2 Obtained by X-ray diffraction measurements (circles) and by dilatometric measurements (dotted lines). Open and closed circles show the processes with decreasing and increasing temperature, respectively. Solid lines are guides for eyes.

responsible for the onset of Mn moments. It is clear that the type of the crystal structure (C15 or C14) is not responsible for it. The possibility of an induced moment by exchange fields from rare-earth moments, which is the origin of Co moments in RCo_2, is also ruled out because YMn_2 has a large moment. Fig. 7 implies that the lattice parameter plays a crucial role in determining whether the Mn atom possesses a magnetic moment or not. The larger lattice parameter makes the 3*d* band width narrower and the density of states higher. Therefore, it is natural that Mn atoms become magnetic in RMn_2 with a large unit cell volume. Anyhow, a small difference in the environment of a Mn atom makes it magnetic with a fairly large moment on one side and nonmagnetic on the other side. In other words, the difference in the

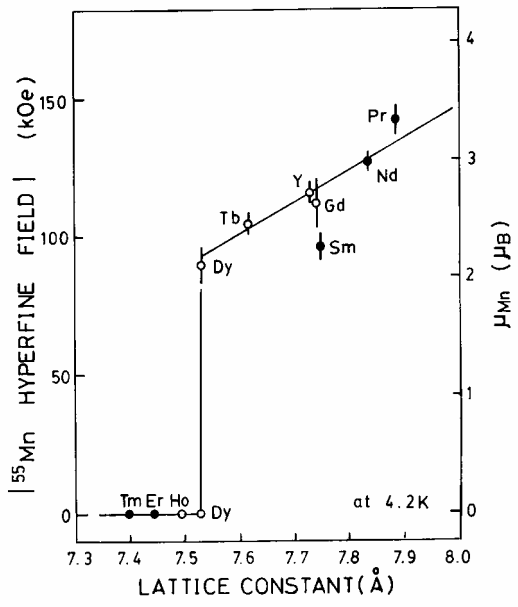

Fig. 7. Relation between the ^{55}Mn hyperfine field. H_{self} and the lattice parameter of RMn_2 at 4.2K. The transferred hyperfine fields from rare-earth moments are subtracted from the observed ones. The effective lattice parameter of C14 compounds (closed circles) is given by $a_{eff}=(\sqrt{3}a^2c)^{1/3}$. The scale for the estimated Mn moment from H_{self} is given on the right-hand side.

free energy between these two states should be very small and, therefore, we can expect many interesting phenomena such as characteristic spin fluctuations.

4.2. Magnetic structures

Before discussing the characteristic spin fluctuations in RMn_2 Series, we summarize the magnetic structures of RMn_2 in the ground state. The antiferromagnetism of YMn_2 suggests a negative interaction between Mn moments. It is likely that the interaction between rare-earth moments is positive because most of RAl_2 and RNi_2 are ferromagnetic and that the R-Mn interaction is negative for heavy rare-earth and positive for light rare-earth elements as observed in RFe_2 and RCo_2 compounds. Any simple magnetic structure such as a ferromagnet or a collinear antiferromagnet does not satisfy these competitive interactions. Therefore, complex magnetic structures are expected if Mn atoms are magnetic.

Fig. 8 shows the temperature dependence of magnetization of $PrMn_2$, $NdMn_2$ and $SmMn_2$, all of which have the C14 structure. The susceptibility of each compound has a sharp peak at the temperature where the thermal expansion curve shows an anomaly, indicating antiferromagnetism of these compounds. Recently, neutron diffraction experiments have been done on $PrMn_2$ and $NdMn_2$ [16]. The magnetic structures have been determined as a complex antiferromagnet with double propagation vectors and in $NdMn_2$ a spin reorientation takes place around 50 K [16]. In both compounds, fairly large lattice distortions to a monoclinic structure have been observed below T_N [17]. The zero-field NMR spectra and the field dependence of spin echo intensity have been measured for these antiferromagnetic compounds [18]. Five lines due to the quadrupole interactions have been observed in the zero-field spectra and the field dependence of each peak is antiferromagnetic.

The magnetic structure of $GdMn_2$ is not yet well understood. The temperature dependence of magnetization looks like a ferromagnet with the Curie temperature of about 40K [19]. The magnetization curve of $GdMn_2$ at 4.2K, however, is not typically ferromagnetic. It does not

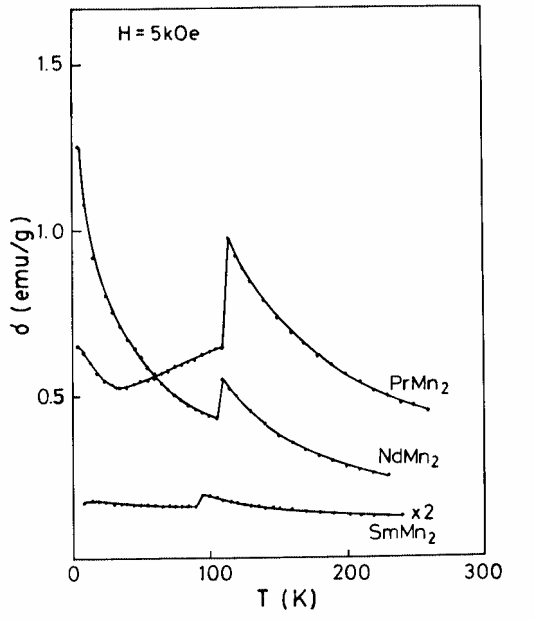

Fig. 8. Magnetization vs. temperature of $PrMn_2$, $NdMn_2$ and $SmMn_2$.

saturate even at 350 kOe [20] and the magnetic moment per unit formula is far below the value for Gd^{3+}, implying a complex magnetic structure such as canted ferromagnetism or helimagnetism. The zero-field NMR spectrum of ^{55}Mn in $GdMn_2$ shows a broad peak with some structures around 120 MHz (fig. 9) [15]. The broadening may be originated in the anisotropic hyperfine fields or the quadrupole interactions. The complex structure of the spectrum, however, cannot be interpreted for a collinear arrangement of Mn moments. The effect of external fields on the NMR spectrum is also not simple (see fig. 9). Although the average resonance frequency increases gradually with increasing field, the shift is much smaller than that expected for a collinear spin arrangement. By analyzing the spectra under external fields, it has been concluded that the directions of Mn moments distribute nearly perpendicular to the total magnetization. A recent neutron diffraction study, being extremely difficult because of the strong neutron absorption by Gd, has shown that, without an applied field, no ferromagnetic component is detected and non-integer magnetic Bragg peaks are observed [16]. These observations imply a helical structure of $GdMn_2$ in the ground state in which Gd moments are easily magnetized up to a limited value by an applied field. Another interesting behavior of $GdMn_2$ is that the magnetization under an applied field disappears around 40K which is far below the Néel temperature of Mn sublattice characterized by the thermal expansion anomaly at 110 K as shown in fig. 10. This behavior was explained as that by cancellation of molecular fields from the antiferromagnetic Mn sublattice, the ferromagnetic Gd sublattice becomes independently paramagnetic around 40 K [19]. The analysis of the specific heat [21], however, has revealed that the magnetic entropy due to Gd moments mainly increases at 110 K but not at 40 K, implying that the Gd sublattice is not paramagnetic between 40 and 110 K but is in a magnetically ordered state.

The magnetic structure of $TbMn_2$ has been determined to be a helimagnet of the modulation period of 8 Å [22]. By applying a field, a metamagnetic transition starts at around 15 kOe [23] and the magnetization per unit formula approaches to the Tb^{3+} value in contrast to $GdMn_2$ [15]. The ferromagnetic phase remains after removing the field. Corresponding to this

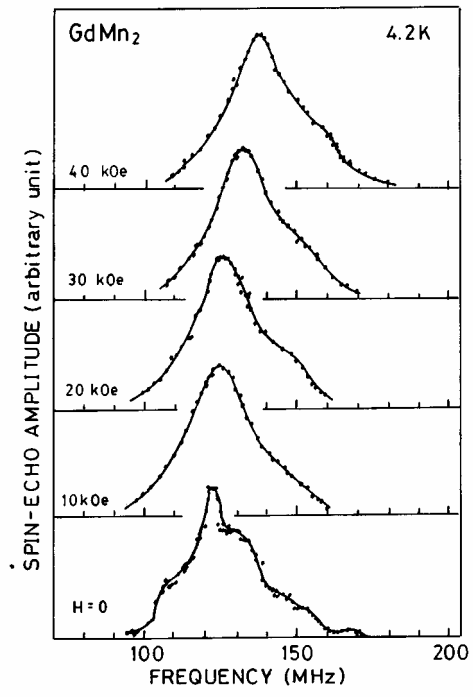

Fig. 9. ^{55}Mn spin-echo NMR spectra of $GdMn_2$ observed under several external fields at 4.2 K.

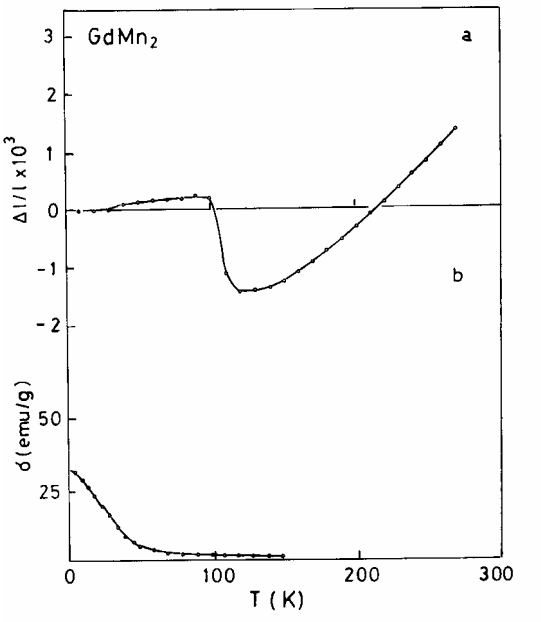

Fig. 10. Thermal expansion curve (a) and temperature dependence of the magnetization at 5 kOe (b) of $GdMn_2$.

process, the ^{55}Mn NMR spectrum shows characteristic changes (fig. 11). In the virgin state, the zero field spectrum consists of a broad single peak without any fine structure. This pattern may be explained as a result of a distribution of anisotropic hyperfine fields and quadrupole interactions due to the helical modulation of Mn moments. The spectra under applied fields show a flat distribution of resonance fields. The center of gravity of the spectra does not change and the width of distribution is proportional to γH. These features are characteristic to an antiferromagnetic powder pattern. The zero-field spectrum after applying the field is quite different from that of the virgin state, having two peaks. One of these peaks was ascribed to the Mn moments aligning parallel to Tb moments and the other to those aligning antiparallel [15]. In order to determine the magnetic structure of $TbMn_2$ under the external field and in the remanent state definitely, precise neutron studies are necessary.

By magnetization measurements of a single

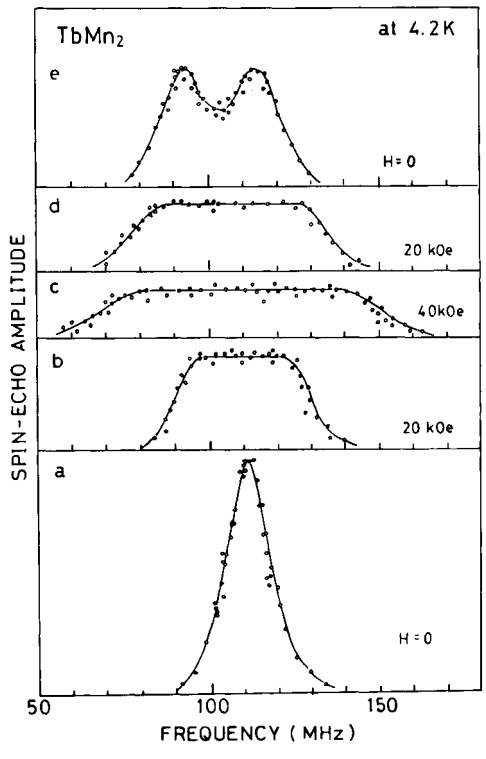

Fig. 11. ^{55}Mn spin-echo NMR spectra of $TbMn_2$ observed under 0, 20, 40 kOe at 4.2 K: in the zero-field cooling state (a), with increasing field (b and c) and with decreasing field (d and e).

crysta, it is claimed that $DyMn_2$ is a canted-ferromagnet where Dy moments orient to one of the (110) directions and adjacent Dy moments align perpendicular to each other [24]. By applying a strong field, the canted structure transforms to a collinear ferromagnet with the easy direction of (110). In the thermal expansion curve, there is no anomaly, indicating the absence of Mn moment. However, there are some unsolved problems in NMR spectra of $DyMn_2$ [15]. The main resonance peak of $DyMn_2$ is the low frequency one which is originated in nonmagnetic Mn atoms. In addition, a weak resonance peak is observed at 73 MHz, which cannot be ascribed to an impurity phase, implying the existence of magnetic Mn atoms. Since $DyMn_2$ locates at the critical position for the onset of Mn moment (see fig. 7), it is presumable that a part of Mn atoms becomes magnetic depending upon their environments. Noting the fact, however, that the C15 structure has only one Mn site, the difference in the environment cannot be a chemical one but should be a magnetic one. Therefore, it is possibly that the magnetic structure is more complicated than so far proposed.

$HoMn_2$ (C15 and C14) and $ErMn_2$ (C14) are simply ferromagnetic [19]. From analyses of the internal fields and from the lack of large thermal expansion anomaly, we believe that Mn atoms are nearly nonmagnetic in these compounds although some neutron diffraction studies conclude the existence of substantial Mn moments in $HoMn_2$ [25].

5. Spin fluctuations in YMn_2 and relate compounds

The Mn moment in RMn_2 compounds is highly unstable and, therefore, it should be very sensitive to the change of external parameter such as pressure or to the substitution of a third element. Actually, the antiferromagnetism of YMn_2 is easily destroyed by a relatively low pressure of 3 kbar [16, 26]. We show the effects of substitution of third elements, and estimate the amplitude of spin fluctuations in YMn_2 and related compounds.

5.1. $Y(Mn_{1-x}M_x)_2$ system

The lattice parameter of $Y(Mn_{1-x}M_x)_2$ is shown in fig. 12. Except for M=Al, the lattice parameter decreases linearly with increasing *x*. In fig 13, the intensity of zero-field NMR signal of ^{55}Mn observed around 120 MHz, which is originated in the magnetic Mn in the antiferromagnetic state, is plotted against *x*. Except for M=Al, the intensity of the signal decreases rapidly with increasing *x*. After the disappearance of the zero-held signal, a paramagnetic NMR signal is detected in the samples such as $Y(Mn_{0.92}Fe_{0.08})_2$, indicating the collapse of Mn moments [27]. Furthermore, the large thermal expansion anomaly observed in YMn_2 disappears. we may regard the spin fluctuations in these materials as of type a or of type b of fig. 2.

On the other hand, the $Y(Mn_{1-x}A1_x)_2$ system, of which lattice parameter increases with increasing x, shows contrastive characters. The resonance frequency of the zero-field NMR remains constant around 120 MHz and its intensity decreases slightly with increasing x. The rate of the decrease, however, is much slower than that of the $Y(Mn_{1-x}Co_x)_2$ and $Y(Mn_{1-x}Fe_x)_2$ systems. No paramagnetic NMR signal was detected in an applied field. These observations indicate that the magnitude of Mn moments in the $Y(Mn_{1-x}Al_x)_2$ system remains constant at 0 K for substitution of Mn by Al. Fig. 14 shows the temperature dependence of the susceptibility of $Y(Mn_{1-x}Al_x)_2$. The χ-*T* curve approaches to the Curie-Weiss type with increasing *x*, indicating a transition from the itinerant antiferromagnetism to the local moment limit [28]. In order to know the temperature dependence of spin fluctuations, we have measured the thermal expansion of $Y(Mn_{1-x}Al_x)_2$ by X-ray diffraction, the results of which are shown in fig. 15 [29]. As seen in the figure, a substitution of Mn by Al gives rise to dramatic changes in the thermal expansion curves as follows. (i) The volume change at T_N decreases with increasing *x* and almost disappears at $x = 0.1$. For $x > 0.1$, the thermal expansion curve does not change so much with Al concentration. (ii) For $x = 0.02$, a discontinuity is still observed at T_N, indicating a first-order phase transition, while the variation

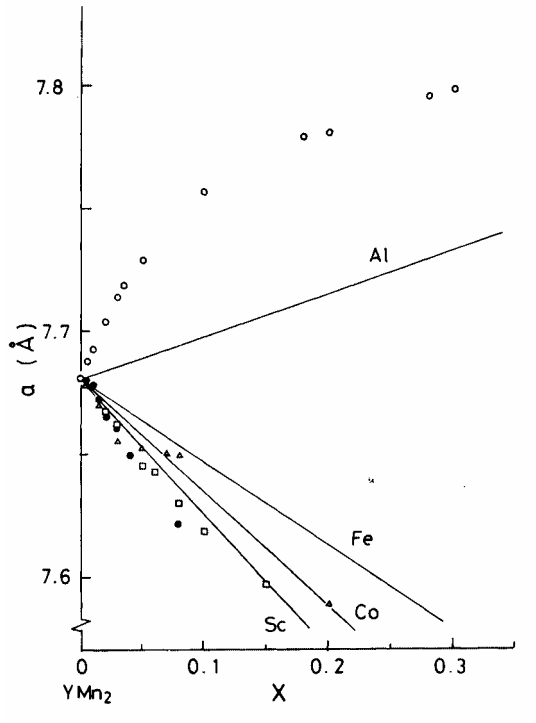

Fig. 12. Lattice parameter of $Y(Mn_{1-x}M_x)_2$ at room temperature (○ : M=Al, □: M=Fe, △: M=Co) and $(Y_{1-x}Sc_x)Mn_2$(●). Solid lines indicate Vegard's law.

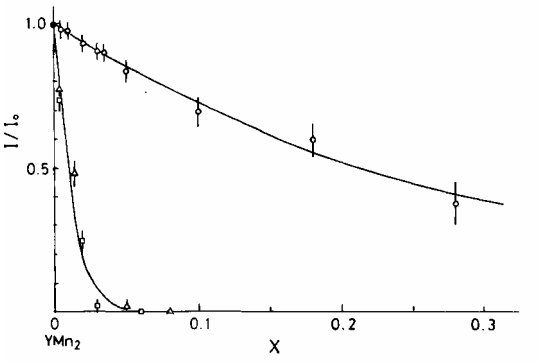

Fig. 13. Relative integrated intensity of ^{55}Mn spectrum of $Y(Mn_{1-x}M_x)_2$ at 1.3 K as a function of x. ○: M=A1, □: M=Fe, △: M=Co.

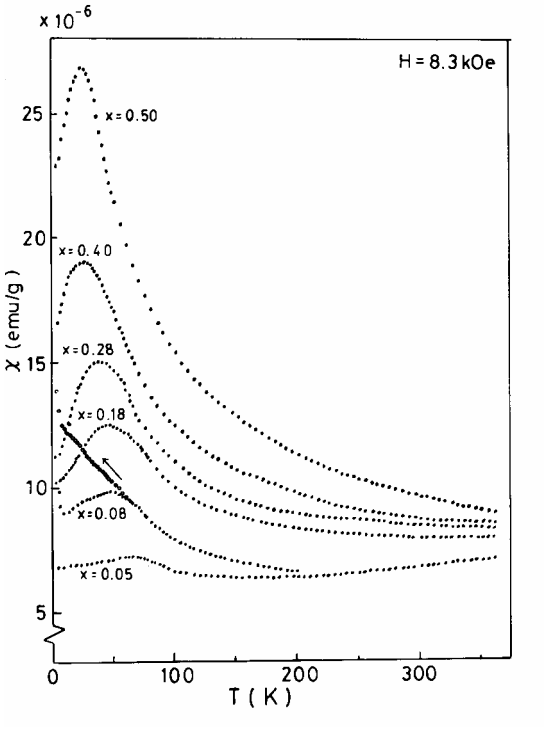

Fig. 14. Temperature dependence of the susceptibility of $Y(Mn_{1-x}Al_x)_2$. Open circles for x=0.08 indicate a field cooling process.

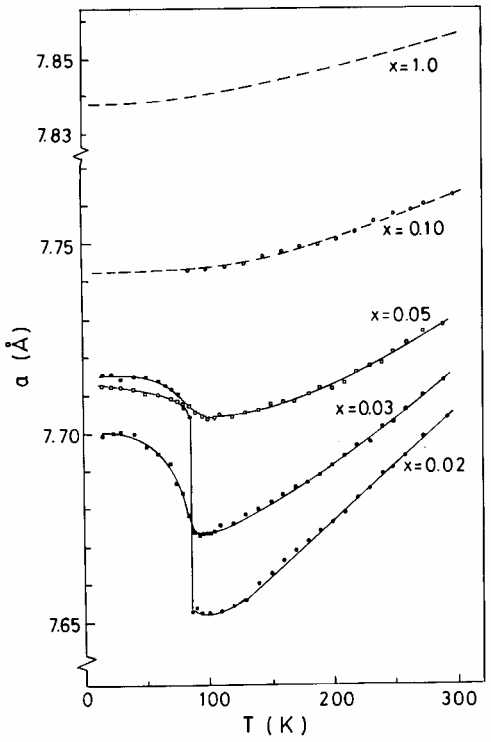

Fig. 15. Thermal expansion curves of $Y(Mn_{1-x}Al_x)_2$ mea sured by either X-ray diffraction (circles and squares) or a dilatometer (broken curves). Full curves are guides for eyes.

of the lattice parameter becomes continuous at T_N for $x \geq 0.03$, indicating a second-order transition. (iii) The TEC above T_N decreases with increasing x and reaches a normal value of about 16×10^{-6}. As clearly shown in fig. 16, the TEC at room temperature is enhanced for $x <$ 0.1.

These observations as well as the concentration dependence of lattice parameter at room temperature can be explained by assuming a characteristic feature of spin fluctuations as shown schematically in fig. 17 as follows. We may write the lattice parameter of $Y(Mn_{1-x}Al_x)_2$ at a given temperature T as

$$a(x, T) = a^0(x, 0) + \Delta a(x, T) + 1/3 \cdot k(1 - x)m_{Mn}^2, \qquad (1)$$

where $a_0(x, 0)$ represents the lattice parameter at 0 K in the hypothetical nonmagnetic state, $\Delta a(x, T)$ is the thermal expansion due to lattice vibrations and k the magnetovolume coupling constant [29].

As shown by the chained line in fig. 17, m_{Mn}^2 at room temperature increases sharply with increasing x for $x < 0.1$. Assuming Vegard's law for the nonmagnetic lattice parameter, that is, for the first and the second terms of eq. (1), we can explain the upward deviation of the lattice parameter at room temperature by the sharp increase of the third term of eq. (1).

From fig. 17 and eq. (1), one can easily understand the decrease of the thermal expansion anomaly at T_N. The enhancement of the TEC above T_N for small x is a result of the recovery of the spin fluctuation amplitude, and the trend of saturation of m_{Mn}^2 at high temperatures gives rise to a decrease of TEC as seen in fig. 4. Since the Mn moment is constant against temperature for $x > 0.1$, the thermal expansion is ascribed only to anharmonic lattice vibrations and exhibits normal behavior.

By using eq. (1), we can estimate m_{Mn}^2 if the first and the second terms and the constant k are correctly given. The first term, $a^0(x, 0)$, can be given by

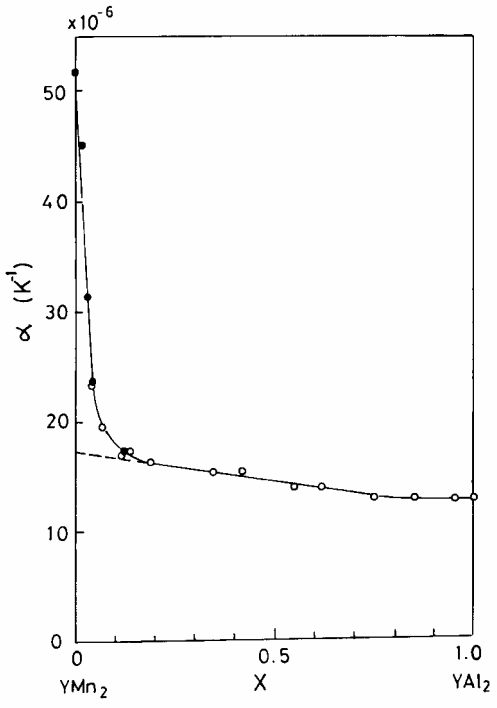

Fig. 16. Concentration dependence of the thermal expansion coefficient of $Y(Mn_{1-x}Al_x)_2$ at room temperature. Full circles are determined by X-ray measurements and open circles b) dilatomeric measurements. The broken line is an extrapolated line from x >0.2.

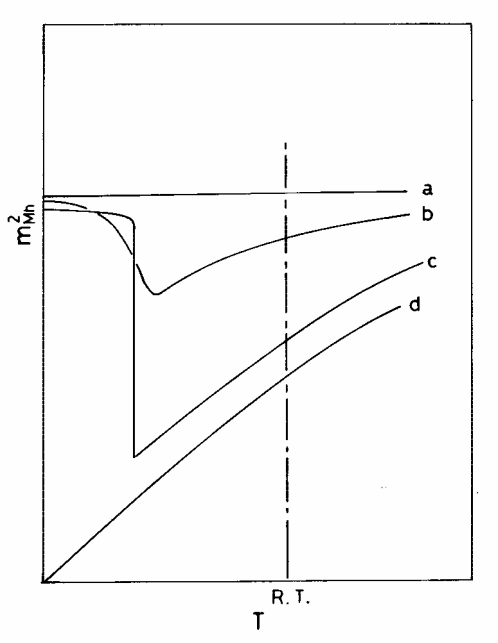

Fig. 17. Schematic features of temperature dependence of the magnitude of the Mn moment in the system $Y(Mn_{1-x}Al_x)_2$, for (a) x>0.1, (b) 0<x<0.1 and (c) x=0, and (d) $Y_{0.97}Sc_{0.03}Mn_2$.

$$a^0(x, 0)= a^0(0, 0)(1 - x)+ a^0(1, 0)x ,$$

where $a^0(0, 0)$ is the lattice parameter of YMn_2 at 0 K in the hypothetical nonmagnetic state, which was obtained by an extrapolation of the thermal expansion curve of YMn_2 from the paramagnetic region. $a^0(1, 0)$ is the lattice parameter of YAl_2 at 0 K, which was estimated from the room temperature lattice parameter and the thermal expansion curve. For an estimation of $\Delta a(x, T)$, we assume that the Mn moment has its full T-independent value over the whole temperature range in the Al-rich region and, therefore, the thermal expansion is due only to lattice vibrations for $x > 0.2$. For $x < 0.2$, we assume that the unenhanced TEC at room temperature lies on the extrapolated line from $x > 0.2$, as shown by the broken line in fig. 16. Using these values and the Debye model, we estimated $\Delta a(x, T)$ for $x < 0.2$. The coupling constant k was estimated from the spontaneous volume magnetostriction and the Mn moment of $2.7\mu_B$ of YMn_2 at 0 K as given:

$$\omega_s(0) = 3[a(0, 0) - a^0(0, 0)]/a^0(0, 0)$$
$$= k(2.7\ \mu_B)^2.$$

we have $\omega_s(0)=5.1 \times 10^{-2}$ and $k=7 \times 10^{-3}/\mu_B^2$.

The estimated Mn moments are plotted against temperature in fig. 18. The Mn moment at low temperatures has an x-independent value of $(2.7 \pm 0.3)\mu_B$, which is consistent with the constant resonance frequency of zero-field NMR. It should be noted that the Mn moment in YMn_2 is reduced to about $1\mu_B$ just above T_N and recovers to $2\mu_B$ at room temperature. Recently, paramagnetic neutron scattering experiments to estimate the Mn moment above T_N have been done on YMn_2 [30, 31]. The magnitude of Mn moment obtained by the neutron scattering is shown in fig. 18 together with that obtained by the thermal expansion. It should be noted that, in spite of many assumptions for the estimations, both results are in good agreement. From these analyses, it becomes evident that a

large amplitude of spin fluctuations is induced thermally above T_N in YMn_2. It is an interesting problem to know the effect of the giant spin fluctuations on other thermodynamic properties near 0 K. We have successfully stabilized the paramagnetic state to 0 K by substituting Y by Sc as will be shown in the next section.

We have shown that the Mn moment is stabilized by substitution of Al for Mn but have not mentioned the ground-state spin structure. The sharp peak in the χ-T curves implies an antiferromagnetic spin ordering for $x \geq 0.05$. However, neutron diffraction of $Y(Mn_{0.95}Al_{0.05})_2$ has revealed that the intensity of magnetic Bragg peaks is notably reduced and they become diffusive, implying the collapse of long-range antiferromagnetic order [29, 32]. Furthermore, we have found that the maximum of the χ-T curves disappears for a field-cooled sample as shown in fig. 14. From these facts, it is likely that the peak in the χ-T curves is due to spin-glass freezing. It is worthwhile to note that the magnetic interactions in YMn_2 are frustrative because any antiferromagnetic structure cannot fully satisfy the negative n.n. Mn interactions because of the tetrahedron arrangement of Mn atoms [14]. It has been pointed out that impurities in a system with frustrative interactions play a similar role as random fields in a usual ferromagnetic system and destroy a periodic spin structure of the system [33]. This system may be a typical one in this situation.

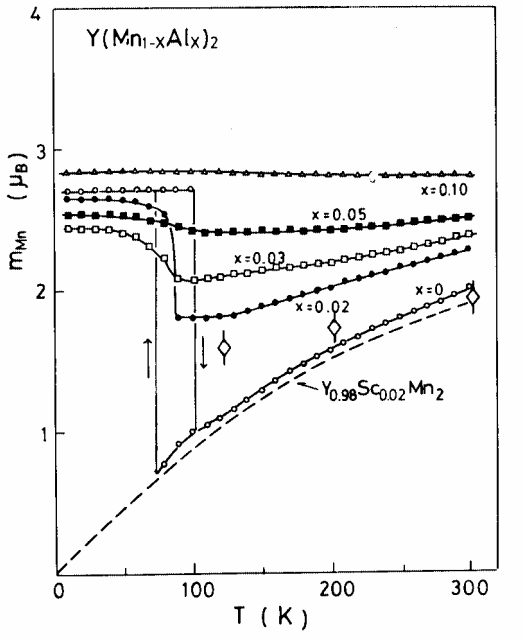

Fig. 18. Temperature dependence of the Mn local moment, m_{Mn}, in the systems $Y(Mn_{1-x}Al_x)_2$ and $Y_{1-x}Sc_xMn_2$ estimated from the analyses of thermal expansion curves. Lozenges indicate m_{Mn} in YMn_2 obtained by neutron scattering[30].

5.2. $(Y_{1-x}Sc_x)Mn_2$: 3d heavy fermion system?

As discussed in a previous section, the substitution of Fe and Co for Mn gives rise to the collapse of Mn moments. The substitution of transition metals for Mn, however, may make the system magnetically inhomogeneous. Actually, the NMR spectra under applied fields are somewhat broad, indicating an existence of weakly magnetic ordering [27]. On the other hand, we can expect a purely nonmagnetic state by the substitution of Y site by a third element with a smaller atomic radius than Y such as Sc because the Mn sublattice is not disturbed. As seen in fig. 12, the lattice parameter of $(Y_{1-x}Sc_x)Mn_2$ decreases with increasing x up to x=0.2, beyond which the C14 phase coexists. The discontinuity in the χ-T curve disappears for $x > 0.02$ indicating the collapse of the antiferromagnetic state [34]. The intensity of zero field NMR spectra sharply decreases with increasing x and disappears for $x > 0.02$. For $x > 0.02$, very sharp resonance peaks are observed in applied field at the frequency of K=0 for both ^{55}Mn and ^{45}Sc as seen in fig. 19, strongly indicating that the system collapses to the complete nonmagnetic state at 4.2 K [35].

Fig. 20 shows the temperature dependence of lattice parameter of $(Y_{1-x}Sc_x)Mn_2$. The lattice expansion due to the antiferromagnetic state disappears for $x > 0.02$. For $0 < x < 0.02$, a coexistence of the antiferromagnetic and paramagnetic phases is observed, indicating that the transition from the antiferromagnetic state to the paramagnetic phase is of the first order with respect to the substitution of Sc for Y.

In contrast to the Al substitution, the slope of the thermal expansion curves is nearly the same as that of YMn_2 above T_N., the enhancement of TEC is still observed, indicating the giant spin fluctuations even at low temperatures. Furthermore, we found that the γ value of

low-temperature specific heat is enormously large as 140 mJ/mol K^2 [36], which is about 10 times as large as the bare density of states [1, 37]. This enhancement of the γ value may also be ascribed to the giant spin fluctuations. Noting these facts, we may say that this compound is a candidate for a heavy fermion system of 3*d* electrons. Actually, it has been found that the temperature dependences of electric resistivity and thermo-electric power of $Y_{0.97}Sc_{0.03}Mn_2$ show a close similarity to those of a typical heavy fermion system such as UPt_3 [38].

In order to detect the spin fluctuations directly, we have carried out paramagnetic neutron scattering experiments using polarized neutron at 8, 120 and 300 K [39]. The characteristic features of the magnetic scattering spectra are as follows: (i) A large amplitude of scattering is observed centered around Q = 1.5 $Å^{-1}$, indicating a strong antiferromagnetic correlation. (ii) The intensity of scattering increases with increasing temperature, indicating that the fluctuations are thermally induced. (iii) At the lowest temperature, 8 K, huge scatterings are still observed,

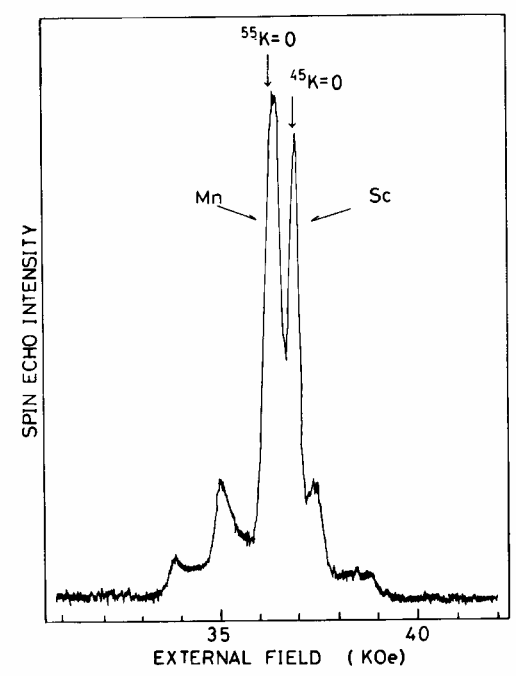

Fig. 19. Recorder trace of the ^{55}Mn and ^{45}Sc spin-echo NMR intensity for $Y_{0.97}Sc_{0.03}Mn_2$ against external field at an operating frequency of 37.915 MHz at 4.2 K.

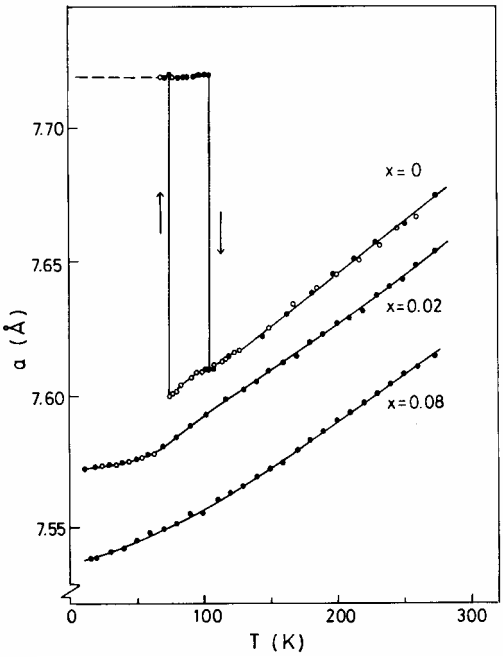

Fig. 20. Temperature dependence of the lattice parameter of $Y_{1-x}Sc_xMn_2$. Full and open circles indicate heating and cooling processes, respectively. Solid curves are guides for eyes.

suggesting strong zero-point fluctuations. These observations strongly suggest that this compound is nearly antiferromagnetic and that giant spin fluctuations play an important role in heavy fermion like behavior.

Acknowledgements

The author would like to thank Professor Y. Nakamura for his advice and encouragement. He is much indebted to Dr. H. Wada, Dr. K. Yoshimura and Mr. H. Nakamura for useful discussions and for experiments.

References

[1] H. Yamada, J. Inoue, K. Terao, S. Kanda and M. Shimizu, J. Phys. **F 14** (1984) 1943.

[2] H. Yamada and M. Shimizu, J. Phys. **F 16** (1986) 1039.

[3] H. Yamada, in this issue.

[4] T. Moriya, J. Magn. Magn. Mat. **14** (1979) 1.

[5] M. Shiga, AIP Conf. Proc. No. 18 (1973) 463.

[6] M. Shiga, J. Phys. Soc. Japan **50** (1981) 2573.
[7] M. Matsunaga, Y. Ishikawa and T. Nakajima, J. Phys. Soc. Japan **51** (1982) 1153.
[8] S. Ogawa, Physica **119B** (1983) 68.
[9] K. Suzuki and Y. Masuda, J. Phys. Soc. Japan **54** (1985) 630.
[10] J.J.M. Franse, Physica **86B** (1977) 283.
[11] M. Shiga, H. Wada and Y. Nakamura, J. Magn. Magn. Mat. **31-34** (1983) 119.
[12] Y. Nakamura, J. Magn. Magn. Mat. **31-34** (1983) 829.
[13] Y. Nakamura, M. Shiga and S. Kawano, Physica **120B** (1983) 212.
[14] R. Ballou, J. Deportes, R. Lemaire, Y. Nakamura and B. Ouladdiaf, J'. Magn. Magn. Mat. **70** (1987) 129.
[15] K. Yoshimura, M. Shiga and Y. Nakamura, J. Phys. Soc. Japan **55** (1986) 3585.
[16] B. Ouladdiaf, Thesis submitted to L'Universite Scientifique *et* Medicale et L'Institut National Polytechnique de Grenoble (1986).
[17] Y. Tagawa, J. Sakurai, Y. Komura, H. Wada, M. Shiga and Y. Nakamura, J. Phys. Soc. Japan **54** (1985) 591.
[18] K. Yoshimura and Y. Nakamura, J. Phys. Soc. Japan **53** (1984) 3611.
[19] S.K. Malik and W.E. Wallace, J. Magn. Magn. Mat. **24** (1981) 23.
[20] H. Wada, K. Yoshimura, M. Shiga, T. Goto and Y. Nakamura, J. Phys. Soc. Japan **54** (1985) 3543.
[21] T. Okamoto, H. Nagata, H. Fujii and Y. Makihara, J. Magn. Magn. Mat. **70** (1987) 139.
[22] L.M. Corliss and J.M. Hastings, J. Appl. Phys. **35** (1964) 1051.
[23] I.Yu. Gaidukova, S.B. Kruglyashov, A.S. Markosyan, R.Z. Levitin, Yu.G. Pastushenkov and V.V. Snegirev, Zh. Eksp. Teor. Fiz. **84** (1983) 1858.
[24] Y. Makihara, Y. Andoh, Y. Hashimoto, H. Fujii, M. Hasuo and T. Okamoto, J. Phys. Soc. Japan **52** (1983) 629.
[25] K. Hardman, J.J. Rhyme, S. Malik and W.E. Wallace, J.Appl. Phys. **53** (1982) 1944.
[26] G. Oomi, T. Terada, M. Shiga and Y. Nakamura, J. Magn. Magn. Mat. **70** (1987) 137.
[27] K. Yoshimura, M. Takigawa, H. Yasuoka, M. Shiga and Y. Nakamura, J. Magn. Magn. Mat. **54-57** (1986) 1075.
[28] M. Shiga, H. Wada, K. Yoshimura and Y. Nakamura, J. Magn. Magn. Mat. **54-57** (1986) 1073.
[29] M. Shiga, H. Wada, H. Nakamura, K. Yoshimura and Y. Nakamura, J. Phys. **F 17** (1987) 1781.
[30] J. Deportes, B. Ouladdiaf and K.R.A. Ziebeck, J. Physique **48** (1987) 1029.
[31] T. Freltoft, P. Boni, G. Shirane and K. Motoya, to appear in Phys. Rev. B.
[32] K. Motoya, J. Phys. Soc. Japan **55** (1986) 3733.
[33] F. Matsubara, J. Phys. Soc. Japan **54** (1985) 1677.
[34] H. Nakamura, H. Wada, K. Yoshimura, M. Shiga, Y. Nakamura, J. Sakurai and Y. Komura, to appear in J. Phys. F.
[35] K. Yoshimura, H. Nakamura, M. Takigawa, H. Yasuoka, M. Shiga and Y. Nakamura, J. Magn. Magn. Mat. **70** (1987) 142.
[36] H. Wada, H. Nakamura, E. Fukami, K. Yoshimura, M. Shiga and Y. Nakamura, J. Magn. Magn. Mat. **70** (1987) 17.
[37] S. Asano and S. Ishida, J. Magn. Magn. Mat. **70** (1987) 39.
[38] J. Sakhrai, private communication.
[39] M. Shiga, H. Wada, Y. Nakamura, J. Deported, R.Ballou and K.R.A. Ziebeck, in preparation.